# Solution of Waveguide Discontinuities by Modal Analysis

ALVIN WEXLER, MEMBER, IEEE

*Abstract*—A general method is presented for analysis of waveguide junctions and diaphragms by summing normal modes of propagation, giving solutions for the resulting scattered modes. Because interaction effects of dominant and higher-order modes between discontinuities are allowed, finite-length obstructions can be studied.

Solutions are found without any prior assumption about the total fields existing at the discontinuities and, as a result, the formulation is applicable to a wide range of problems. The technique proves to be simple and is ideally suited to computers, involving mainly the solution of sets of simultaneous linear equations.

Thick and thin symmetrical bifurcations of a rectangular guide are studied. Forward-scattered mode amplitudes and input admittances are calculated, the computed admittance of the thin bifurcation is compared with well-known results, and transverse field patterns on both sides of the junction are plotted, thus showing the accuracy of the match.

The results of a finite-length bifurcation by a thick vane are presented for a range of lengths, the parameters of the equivalent $T$ network being given in each case. For very short lengths, the problem corresponds to an inductive strip across the guide.

## I. Introduction

VERY FEW waveguide discontinuities have been solved exactly, and these have been accomplished by integral transform techniques [1]. Other integral equation formulations, solved by quasi-static approximations, were reviewed by Lewin [2]. Although there is hope that some restrictions may eventually be alleviated if new ways of dealing with integral equations are found, the outlook is not particularly bright. Collin [3] presents examples illustrating the use of variational techniques. But the method as outlined requires much mathematical innovation when applied directly to particular problems. Other approaches employing static approximations and perturbational methods are very approximate and are usually unacceptable for the broad class of problems encountered in practice.

In the modal analysis method, the amplitudes of normal modes are chosen so as to satisfy boundary conditions at the discontinuity. Because the modal approach is direct and conforms closely to physical reality, it should have the widest application. The method gives excellent estimates to the aperture fields and scattered modes, and should be of particular value to multimode propagation studies, e.g., multimode techniques applied to aerial improvement [4]. Objections of slow convergence and involved numerical work are not particularly significant to digital computers, and so demand is increasing for a general and convenient formulation rather than for economy in computing effort. It is, therefore, the purpose of this paper to present a general method of normal mode summation, to renew interest in the technique that has never been fully exploited, and to argue the case for a complete change of emphasis in the solution of waveguide discontinuity problems.

Manuscript received September 17, 1966; revised May 8, 1967.

The author is with the Department of Electrical Engineering, University of Manitoba, Winnipeg, Canada.

## II. Description of the Problem

Consider two uniform cylindrical waveguides having different cross sections and distributions of enclosed electrical properties. The junction formed by joining them end-to-end, with axial lines parallel, can be described as a function of two transverse coordinates $u_1$ and $u_2$. Boundary conditions, continuity of transverse fields through all apertures and zero tangential electric field at conducting obstacles, are satisfied by a suitable infinite series of modes appropriate to each side of the junction. If the modes of propagation in both guides and the scattering coefficients of succeeding discontinuities are known, the properties of the junction may be computed. The problem is to find how power is apportioned between the various scattered modes.

The transverse fields of each mode may be written as

$$\hat{e}_i(u_1, u_2, z) = a_i \bar{e}_i(u_1, u_2) \cdot e^{\pm \gamma_i z} \tag{1}$$

and

$$\hat{h}_i(u_1, u_2, z) = a_i \bar{h}_i(u_1, u_2) \cdot e^{\pm \gamma_i z}. \tag{2}$$

The sign of the exponent is fixed by the propagating direction. $\hat{e}_i$, $\hat{h}_i$, and $\gamma_i$ are the transverse vector functions and propagation constant of the $i$th mode. If not known explicitly, they can often be derived numerically [5]. Factors $a_i$ are the mode coefficients which, along with the reflection factor $\rho$ of the incident mode, are to be determined. Modes are numbered in an arbitrary sequence, the variables $i$, $j$, $k$, $m$, $n$, and $r$ being reserved for this purpose. In general, the fields must be described in a piecewise fashion, e.g., Fig. 1.

A waveguide cross section consists of a conducting boundary enclosing any distribution of magnetic, dielectric, and perfectly conducting regions. For our purposes, a waveguide boundary is defined as the perfectly conducting periphery containing all permeable regions only. Thus, for example, the cross-section boundary of a coaxial line is the inner wall of the outer conductor and the outer wall of the inner one.

Three classes of discontinuity, consisting of the following situations, must be considered: 1) the projection of the guide boundary nearer the klystron completely encompasses the guide boundary following the junction (Section

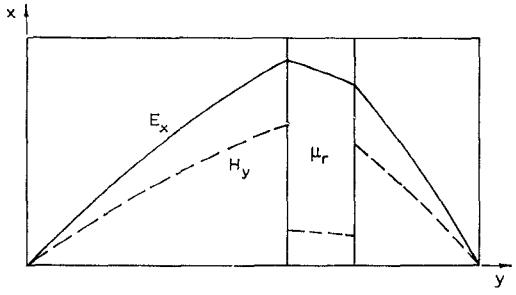


Fig. 1. A possible TE transverse-field configuration in a magnetic slab-loaded waveguide.

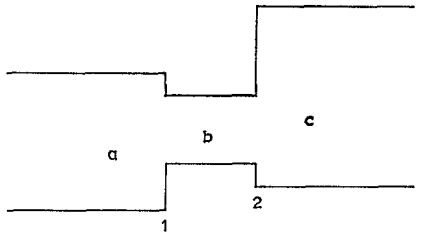


Fig. 2. Three waveguides with higher-order mode coupling between junctions.

III); 2) the guide nearer the klystron is contained within the projection of the guide boundary following the junction (Section IV); and, the remaining possibility, 3) neither guide boundary can be contained within the other (Section V). Classes 1) and 2) include coincident boundaries as a special case.

## III. Boundary Reduction

Fig. 2 represents part of a general waveguide system consisting of three dissimilar guides $a$, $b$, and $c$. The junctions are numbered 1 and 2. Consider a mode $i=1$ emanating from a matched source in $a$ and impinging on waveguide $b$ at $z=0$. The coefficient of this mode is $a_1$, those for the back-scattered modes are $a_2, a_3, \cdots, a_i, \cdots$, and in an anisotropic guide $\rho a_1$ as well. Taking $\bar{\mathscr{E}}$ to be the total transverse electric-field vector function within the aperture at the discontinuity, the field expanded in terms of modes just to the left of junction 1 is

$$\bar{\mathscr{E}} = (1 + \rho)a_1\bar{e}_{a1} + \sum_{i=2}^{\infty} a_i\bar{e}_{ai}. \tag{3}$$

Subscript $a$ denotes quantities relative to the first waveguide. Similarly, the total magnetic field may be expressed by

$$\bar{\mathscr{H}} = (1 - \rho)a_1\bar{h}_{a1} - \sum_{i=2}^{\infty} a_i\bar{h}_{ai}. \tag{4}$$

In many cases, such as modes in the slab-loaded waveguide of Fig. 1 and hybrid modes in rod-loaded circular guides, unique wave admittances cannot be defined. Thus, for complete generality, the transverse electric and magnetic fields are expressed independently.

Refer again to Fig. 2. The aperture fields at $z=0$ will now be expressed in terms of modes in $b$. If waveguide $b$ is matched, the transverse electric-field pattern of mode $j$ is given by $b_j\bar{e}_{bj}$. However, each transmitted evanescent or propagating mode $j$ reaching junction 2 partially reflects and scatters power into other modes $k$, some of which return to junction 1. Therefore, it is necessary to account for these returned waves, as well as for the positively directed ones, when summing modes.

Scattering coefficients are used to relate the amplitudes and phases of modes transmitted past junction 1 to those reflected from junction 2. Consider waveguide $b$ to be excited from junction 1 by a single forward wave $j$ whose coefficient is unity, i.e., $b_j=1$ at junction 1. Then, scattering coefficients $s_{jk}$ are defined as equal to mode coefficients $b_k$, of the back-scattered waves $k$, transformed in amplitude and phase to junction 1 from 2. This is repeated for all $j$. Clearly, junction 2 must be solved before junction 1.

Multiplying $b_j$ by $s_{jk}$ gives the contribution of $j$ to $k$ as seen at junction 1. Because each forward-propagating mode $j$ has an infinity of back-scattered modes $k$ of the form $s_{jk}b_j\bar{e}_{bk}$ associated with it, the total transverse electric and magnetic fields just to the right of junction 1 result by summing over all $j$ and $k$. This gives

$$\bar{\mathscr{E}} = \sum_{j=1}^{\infty} b_j(\bar{e}_{bj} + \sum_{k=1}^{\infty} s_{jk}\bar{e}_{bk}) \tag{5}$$

and

$$\bar{\mathscr{H}} = \sum_{j=1}^{\infty} b_j(\bar{h}_{bj} - \sum_{k=1}^{\infty} s_{jk}\bar{h}_{bk}). \tag{6}$$

Boundary conditions to be satisfied at the discontinuity are as follows: transverse electric and magnetic fields must be continuous across the aperture, and electric field tangential to the conducting obstacle must vanish. The single boundary condition is sufficient at a conducting surface.

Let $m$ be any mode number in waveguide $a$. In all uniform guides with reflection symmetry and perfectly conducting walls, the following orthogonality relation [6] holds for nondegenerate modes:

$$\int_a \bar{e}_{ai} \times \bar{h}_{am} \cdot \bar{u}_z \, ds = 0 \tag{7}$$

when $i \neq m$. The surface integral extends over the entire cross section of the waveguide $a$. Degenerate modes should be orthogonalized by the Gram–Schmidt procedure [7].

Take the cross product of (3) with $\bar{h}_{am}$ and integrate over the cross section of waveguide $a$. Assuming orthogonality of modes and substituting (5) for the (as yet) unknown aperture field $\bar{\mathscr{E}}$, thus employing the continuity condition for transverse electric fields, we get

$$(1 + \rho)a_1 \int_a \bar{e}_{a1} \times \bar{h}_{a1} \cdot \bar{u}_z \, ds = \sum_{j=1}^{\infty} b_j \Big( \int_b \bar{e}_{bj} \times \bar{h}_{a1} \cdot \bar{u}_z \, ds + \sum_{k=1}^{\infty} s_{jk} \int_b \bar{e}_{bk} \times \bar{h}_{a1} \cdot \bar{u}_z \, ds \Big) \tag{8}$$

when $m=1$, and

$$a_m \int_a \bar{e}_{am} \times \bar{h}_{am} \cdot \bar{u}_z \, ds = \sum_{j=1}^{\infty} b_j \left( \int_b \bar{e}_{bj} \times \bar{h}_{am} \cdot \bar{u}_z \, ds + \sum_{k=1}^{\infty} s_{jk} \int_b \bar{e}_{bk} \times \bar{h}_{am} \cdot \bar{u}_z \, ds \right) \quad (9)$$

when $m \neq 1$. Because $\bar{\mathscr{E}}$ exists over the aperture only and vanishes elsewhere, the integrals on the right-hand sides of (8) and (9) are taken over $b$. This completes the electric-field boundary conditions.

Now, take the cross product of (4) with $\bar{e}_{bn}$ and integrate over the cross section of waveguide $b$. Substituting (6) for the unknown aperture field $\bar{\mathscr{H}}$, and using the orthogonality relation

$$\int_b \bar{e}_{bn} \times \bar{h}_{bj} \cdot \bar{u}_z \, ds = 0 \quad (10)$$

for nondegenerate modes when $n \neq j$, we find that

$$(1-\rho) a_1 \int_b \bar{e}_{bn} \times \bar{h}_{a1} \cdot \bar{u}_z \, ds - \sum_{i=2}^{\infty} a_i \int_b \bar{e}_{bn} \times \bar{h}_{ai} \cdot \bar{u}_z \, ds = \left( b_n - \sum_{j=1}^{\infty} b_j s_{jn} \right) \int_b \bar{e}_{bn} \times \bar{h}_{bn} \cdot \bar{u}_z \, ds. \quad (11)$$

Continuity of transverse magnetic field was used in the derivation of (11).

Changing the index $m$ to $i$ in (9), substituting it into (11) so as to eliminate $a_i$, and rearranging, we get

$$\rho \int_b \bar{e}_{bn} \times \bar{h}_{a1} \cdot \bar{u}_z \, ds + \sum_{j=1}^{N} \frac{b_j}{a_1} \sum_{i=2}^{M} \frac{\int_b \bar{e}_{bj} \times \bar{h}_{ai} \cdot \bar{u}_z \, ds + \sum_{k=1}^{N} s_{jk} \int_b \bar{e}_{bk} \times \bar{h}_{ai} \cdot \bar{u}_z \, ds}{\int_a \bar{e}_{ai} \times \bar{h}_{ai} \cdot \bar{u}_z \, ds} \int_b \bar{e}_{bn} \times \bar{h}_{ai} \cdot \bar{u}_z \, ds + \left( \frac{b_n}{a_1} - \sum_{j=1}^{N} \frac{b_j}{a_1} s_{jn} \right) \int_b \bar{e}_{bn} \times \bar{h}_{bn} \cdot \bar{u}_z \, ds = \int_b \bar{e}_{bn} \times \bar{h}_{a1} \cdot \bar{u}_z \, ds; \quad (12)$$

and from (8),

$$\rho \int_a \bar{e}_{a1} \times \bar{h}_{a1} \cdot \bar{u}_z \, ds - \sum_{j=1}^{N} \frac{b_j}{a_1} \left( \int_b \bar{e}_{bj} \times \bar{h}_{a1} \cdot \bar{u}_z \, ds + \sum_{k=1}^{N} s_{jk} \int_b \bar{e}_{bk} \times \bar{h}_{a1} \cdot \bar{u}_z \, ds \right) = - \int_a \bar{e}_{a1} \times \bar{h}_{a1} \cdot \bar{u}_z \, ds. \quad (13)$$

For practical reasons, the infinite series were truncated at $M$ and $N$ which signify the number of modes in waveguides $a$ and $b$, respectively. Equation (12) generates $N$ linear equations where $n=1, 2, \cdots, N$ and (13) supplies one equation. There are $N+1$ unknowns ($b_1/a_1$, $b_2/a_1$, $\cdots$, $b_n/a_1$, $\cdots$, $b_N/a_1$ and $\rho$), and so the system of equations may be solved. For complicated problems (e.g., junctions between rectangular and circular guides or between guides slab-loaded differently, etc.), the integrations in (12) and (13) should be performed numerically [8].

By rewriting (9), the coefficients of the back-scattered modes in guide $a$ may be found. Therefore,

$$\frac{a_i}{a_1} = \frac{\sum_{j=1}^{N} \frac{b_j}{a_1} \left( \int_b \bar{e}_{bj} \times \bar{h}_{ai} \cdot \bar{u}_z \, ds + \sum_{k=1}^{N} s_{jk} \int_b \bar{e}_{bk} \times \bar{h}_{ai} \cdot \bar{u}_z \, ds \right)}{\int_a \bar{e}_{ai} \times \bar{h}_{ai} \cdot \bar{u}_z \, ds}, \quad (14)$$

where $i \neq 1$. Terms previously formed by the Gram–Schmidt orthogonalization procedure should now be decomposed into normal waveguide modes, thus completing the study of the junction.

By using (11) in place of (12), it is possible to solve for $\rho$, $b_j/a_1$, and $a_i/a_1$ all at the same time. This procedure has two disadvantages: 1) the computer store requirement approximately quadruples (assuming that $M$ and $N$ are about the same size); and 2) as the amount of computing is proportional to the cube of the number of unknowns, the work increases by eight times. It is certainly preferable to use (12) and then to find the $a_i/a_1$ through (14).

## IV. Boundary Enlargement

This is the complement of the problem discussed in Section III. Many of the comments made previously are applicable here as well.

Call the first, and smaller, guide $a$ and the larger one $b$. Equations (3) through (6) describe the fields at the junction as before.

The derivation of the simultaneous equations is almost identical to that of Section III. Briefly, cross-multiply (6) by $\bar{e}_{am}$ and integrate over the cross section of $a$. Express the aperture field by (4). Note that, as in (8) and (9), two cases occur: $m=1$ and $m \neq 1$. Also, cross-multiply (5) by $\bar{h}_{bn}$ and integrate over the cross section of $b$, substituting (3) for $\bar{\mathscr{E}}$. Assume orthogonality, and after some algebraic manipulation, the following equations result:

$$\rho \int_a \bar{e}_{a1} \times \bar{h}_{bn} \cdot \bar{u}_z \, ds - \sum_{j=1}^{N} \frac{b_j}{a_1} \sum_{i=2}^{M} \frac{\int_a \bar{e}_{ai} \times \bar{h}_{bj} \cdot \bar{u}_z \, ds - \sum_{k=1}^{N} s_{jk} \int_a \bar{e}_{ai} \times \bar{h}_{bk} \cdot \bar{u}_z \, ds}{\int_a \bar{e}_{ai} \times \bar{h}_{ai} \cdot \bar{u}_z \, ds} \int_a \bar{e}_{ai} \times \bar{h}_{bn} \cdot \bar{u}_z \, ds$$

$$- \left( \frac{b_n}{a_1} + \sum_{j=1}^{N} \frac{b_j}{a_1} s_{jn} \right) \int_b \bar{e}_{bn} \times \bar{h}_{bn} \cdot \bar{u}_z \, ds = - \int_a \bar{e}_{a1} \times \bar{h}_{bn} \cdot \bar{u}_z \, ds, \tag{15}$$

where $n = 1, 2, \cdots, N$;

$$\rho \int_a \bar{e}_{a1} \times \bar{h}_{a1} \cdot \bar{u}_z \, ds + \sum_{j=1}^{N} \frac{b_j}{a_1} \left( \int_a \bar{e}_{a1} \times \bar{h}_{bj} \cdot \bar{u}_z \, ds - \sum_{k=1}^{N} s_{jk} \int_a \bar{e}_{a1} \times \bar{h}_{bk} \cdot \bar{u}_z \, ds \right) = \int_a \bar{e}_{a1} \times \bar{h}_{a1} \cdot \bar{u}_z \, ds; \tag{16}$$

and

$$\frac{a_i}{a_1} = \frac{- \sum_{j=1}^{N} \frac{b_j}{a_1} \left( \int_a \bar{e}_{ai} \times \bar{h}_{bj} \cdot \bar{u}_z \, ds - \sum_{k=1}^{N} s_{jk} \int_a \bar{e}_{ai} \times \bar{h}_{bk} \cdot \bar{u}_z \, ds \right)}{\int_a \bar{e}_{ai} \times \bar{h}_{ai} \cdot \bar{u}_z \, ds}, \tag{17}$$

where $i \neq 1$. The system of $N+1$ linear equations, defined by (15) and (16), may be solved for $b_1/a_1, b_2/a_1, \cdots, b_N/a_1$ and $\rho$. The back-scattered modes $a_i/a_1$ can then be found from (17).

## V. Systems of Connected Waveguides

Fig. 2 depicts part of a system in which interaction of dominant and higher-order modes between discontinuities occurs. As we have seen, if power flows from the left, it is necessary to know the scattering properties of junction 2 before solving the problem at junction 1. Similarly, before analyzing junction 2, the scattering properties of any discontinuity farther down the guide must be known. Ultimately, analysis must begin at a simple termination, such as a matched or single-mode guide or a short circuit which causes independent reflection of each mode incident upon it, regardless of the amplitude and phase of any other.

If the length $l$ of a particular waveguide is small, many modes generated at one junction, figure in the field summation at the other. In other words, higher-order mode coupling occurs. Choose a finite number of modes in the waveguide consisting of the lowest-order modes likely to be set up at either junction.

As indicated earlier, the variable $i = 1$ is not reserved for any particular mode but is allowed to represent any mode presumed incident on a junction. If $r$ is the mode incident on say junction 1, then $\rho_r$ is its reflection factor and $a_i/a_r$, with $i \neq r$, denotes the $M-1$ coefficients of other back-scattered modes. These are all found as previously described. Therefore, $M$ scattering coefficients of junction 1, as defined at the next junction towards the klystron, are given by

$$\begin{aligned} S_{ri} &= \frac{a_i}{a_r} e^{-(\gamma_i + \gamma_r)l} \qquad i \neq r, \\ &= \rho_r e^{-2\gamma_r l} \qquad i = r \end{aligned} \tag{18}$$

thus including amplitude and phase change of both incident and scattered modes between junctions. Consider each mode $r = 1, 2, \cdots, M$, in turn, to be independently incident on the junction, and solve the resulting system of equations each time. In this way, all $M^2$ scattering coefficients are found.

Junctions can be represented by $T$, $\pi$, and transformer networks [9], [10]. To evaluate the equivalent circuit, three determinations of the input admittance $y'$ as a function of a load in guide $c$ are generally required.

### A. Diaphragms and Offset Waveguides

Refer to Fig. 2. Clearly, as the length of waveguide $b$ decreases, the coupling between modes generated at both junctions becomes more pronounced and we have an iris between two offset guides or, as a special case, simply two offset guides. In the study of diaphragms, it is necessary to match fields through the windows. However, it is incorrect to equate both sets of waveguide modes across the plane of the diaphragm, as this will not ensure zero transverse electric field at the conducting surfaces. By treating the diaphragm as a special case of a three-waveguide system, this problem does not arise. Furthermore, this method does not require any prior assumption as to the total field within the window. It is only necessary to know the form of the normal modes in the waveguide defined by the aperture shape.

### B. Multiple-Guide Junctions

Fig. 3 typifies a class of multiple-guide junctions that this method can accommodate. A particular problem is the analysis of selective launching of modes into a large guide $b$ by controlling the amplitude and phase of modes in $a$ and $a'$. This problem is a significant one in the design of multimode aerials [4].

Briefly, the method is as follows. Think of the system to the left of the junction in Fig. 3 as one composite waveguide rather than as a number of guides. The modes in this composite system are defined in a special way. We define a set to conform to the interior of one of the constituent guides,

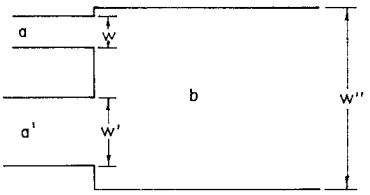


Fig. 3. A multiple-guide junction.

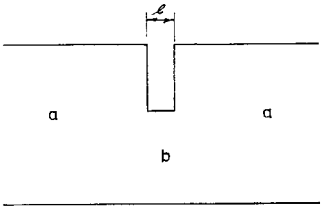


Fig. 4. A thick, symmetrical, inductive iris.

say $a$; elsewhere in the cross section these modes have zero field. Similarly, another set is defined to suit the other guide $a'$, this time with no field over the first aperture and intervening region. These modes are denoted $i=1, 2, \cdots, M$, where $M$ is the total number of modes assumed in both $a$ and $a'$. It is this double set that forms the normal and complete mode system in the composite waveguide. Once modes are defined in this way, it is of no consequence to the matching procedure that they belong to electrically isolated guides.

Now, consider excitation only from $a$ by mode $ir$. This mode will partially reflect into $a$, and other back-scattered modes will be generated, some traveling into $a$ and others into $a'$. Mode coefficients are found by solving the set of simultaneous equations. The problem must then be repeated with excitation from $a'$ and the resulting fields found by superposition.

The reverse situation, with a mode in the large guide impinging on the smaller guides, is handled similarly. The bifurcation, discussed in Section VI, is one problem of this type and the approach is described there.

### C. Symmetry Considerations

Considerable simplification occurs when discontinuities exhibit certain symmetries and are either symmetrically or antisymmetrically excited. For example, the iris in Fig. 4 is symmetrical about a transverse plane. If both ports are excited symmetrically, an open circuit appears at the central plane; antisymmetrical excitation produces a short circuit. Under these conditions, only pure reflection occurs at the central plane, and so $s_{jk}=0$ when $j\neq k$. $s_{jj}$ is given simply by

$$s_{jj} = \frac{1 - y'_{bj}}{1 + y'_{bj}}. \tag{19}$$

$y'_{bj}$ is the normalized input admittance of the $j$th mode in $b$ at the discontinuity, distance $l/2$ from the symmetry plane.

Two parameters are sufficient to specify the equivalent network of such discontinuities. For example, the upper-arm impedances of the equivalent $T$ network are both given by $Z_{11}-Z_{12}$ and the common branch by $Z_{12}$. The computed input impedance, with symmetrical excitation, yields $Z_{11}+Z_{12}$, and that with antisymmetrical excitation gives $Z_{11}-Z_{12}$.

## VI. Numerical Examples

The bifurcation of a rectangular waveguide by a thin vane is one of the few junction problems that have been solved rigorously. As a check on the theory just developed, it will be solved by the modal analysis method. Thick, semi-infinite and finite-length bifurcations will also be investigated. These examples serve to indicate the general approach and illustrate some practical difficulties.

### A. H-Plane Bifurcation

Fig. 5 shows a rectangular waveguide loaded with a thick, perfectly conducting vane. $y$-coordinate dimensions are normalized with respect to the broad dimension $w$. Assuming excitation by an $H_{01}$ mode, only symmetrical modes are generated at the discontinuity. Transverse field patterns of the two lowest-order modes in the bifurcated guide $b$ are shown and are seen to be $H_{01}$ and $H_{03}$ modes deformed by the vane. Modes in $a$ are the usual ones in an empty rectangular guide. Note that this is a boundary-reduction problem.

Expressions for the transverse fields in guide $a$ are

$$\bar{e}_{ai} = \bar{u}_x \sin (p\pi y/w). \tag{20}$$

and

$$\bar{h}_{ai} = \bar{u}_y y_{ai} \sin (p\pi y/w). \tag{21}$$

The wave admittance of the $i$th mode is

$$y_{ai} = \sqrt{\frac{\varepsilon_0}{\mu_0}} \sqrt{1 - \left(\frac{p\lambda_0}{2w}\right)^2}. \tag{22}$$

Modes are numbered consecutively, i.e., $i=1, 2, \cdots, M$, and so

$$p = 2i - 1, \tag{23}$$

thus giving only symmetrical modes when substituted into (20) and (21).

In the left-hand region of waveguide $b$ the transverse fields are

$$\bar{e}_{bj} = \bar{u}_x \sin\left(\frac{2q\pi y/w}{1 - t/w}\right) \tag{24}$$

and

$$\bar{h}_{bj} = \bar{u}_y y_{bj} \sin\left(\frac{2q\pi y/w}{1 - t/w}\right). \tag{25}$$

Equations (24) and (25) hold in the range

$$0 < y/w < 0.5(1 - t/w)$$

and are zero across the vane. Substitute $(1-y/w)$ for $y/w$ when $0.5(1+t/w)<y/w<1$. The admittance of the $j$th mode is

$$y_{bj} = \sqrt{\frac{\varepsilon_0}{\mu_0}} \sqrt{1 - \left(\frac{q\lambda_0/w}{1 - t/w}\right)^2}. \tag{26}$$

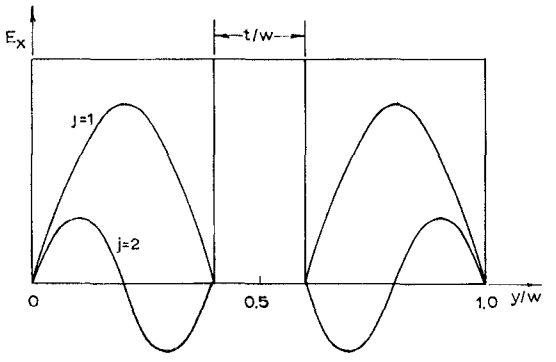


Fig. 5. Transverse fields of the two lowest-order TE modes in a centrally bifurcated rectangular guide.

Here, we have

$$q = j, \tag{27}$$

where $j = 1, 2, \cdots, N$. When calculating $y_{ai}$ and $y_{bj}$, take the positive root when real and the negative imaginary root when imaginary.

If the vane were not central, one set of modes would have to be defined to conform to the interior of one of the partitioned guides with zero field elsewhere. Similarly, another set would have to be defined for the other section. This is similar to the multiple-guide input discussed in Section V. For the symmetrical problem, however, each mode has to be defined over both apertures. Otherwise, two columns of the matrix representing (12) and (13) will be identical, and the system will then be singular.

Referring to (12) and (13), it is seen that the following three integrals are required:

$$\int_a \bar{e}_{ai} \times \bar{h}_{ai} \cdot \bar{u}_z \, ds = 0.5 w y_{ai} \tag{28}$$

$$\int_b \bar{e}_{bj} \times \bar{h}_{bj} \cdot \bar{u}_z \, ds = 0.5 w y_{bj} (1 - t/w), \tag{29}$$

and

$$\int_b \bar{e}_{bj} \times \bar{h}_{ai} \cdot \bar{u}_z \, ds = 0.5 w y_{ai} (1 - t/w) \cdot [\sin(f)/f - \sin(g)/g], \tag{30}$$

where

$$f = [0.5p(1 - t/w) - q]\pi \tag{31}$$

and

$$g = [0.5p(1 - t/w) + q]\pi. \tag{32}$$

The factor $w$ is common to all terms in (12) and (13), and so it may be deleted. As all fields are uniform along $x$, the integrations above were performed only with respect to $y$. Having evaluated these integrals, all the analysis required is completed. This is a particularly simple problem, the $s_{jk}$ terms vanishing due to the infinite length of the bifurcated guide.

Cases $t/w = 0$ and 0.2 were studied with the frequency parameter $w/\lambda_0 = 0.7$. Integrals (28) to (30) were computed and substituted into (12) and (13) as required. The same number of modes were employed in each guide, i.e., $M = N$. The resulting set of simultaneous linear equations was solved by standard Gaussian reduction and back-substitution techniques [11].

Forward- and back-scattered mode coefficients were computed and, from the reflection factor, the normalized input admittance

$$y' = \frac{1 - \rho}{1 + \rho} \tag{33}$$

was found. $y'$ is tabulated in Table I as a function of different expansion sizes for the thick and thin bifurcation. Results of an exact analysis of the thin-vane case, which uses a transform method, are plotted by Marcuvitz [12]. He gives the resulting shift in the null point, and from it the normalized admittance was calculated to be $y' = -j2.416$. On this basis it is seen that the forty-mode expansion is less than 0.05 percent in error. Even with only ten modes the error is less than 1 percent. Also, corresponding computations for a vane with normalized thickness $t/w = 0.2$ are given. An exact solution is not known for this case, and so a comparison is not available. However, the rate of convergence is seen to be equally rapid.

In Table II the first five forward-scattered mode coefficients, normalized with respect to that of the incident mode $i = 1$, are presented for $t/w = 0$. It is clear that the apportionment of power between scattered modes can be closely calculated. For example, there is little difference in the computed $b_j/a_1$ values between the twenty- and forty-mode cases. Coefficients $b_j/a_1$ for lower-order modes are known to a higher accuracy than the remaining terms. This inaccuracy in the last few terms, due to an attempt to compensate for the missing modes, may be seen in the $N = 5$ case where $j = 5$ is the last mode of the finite series.

As a reasonable approximation, take $N = 40$ to furnish almost exact results in comparison to $N = 10$. On this basis, $b_1/a_1$, $b_2/a_1$, and $b_3/a_1$ (for $N = 10$) are known to within errors of 0.5, 2, and 4 percent, respectively. It is difficult to assess just how accurate the $N = 40$ values are, but they are probably of a very high order. Phase angles converge very

rapidly. For this particular problem, all modes in a given solution have the same phase at the discontinuity, except for 180° phase reversals. Similar comments apply to the back-scattered coefficients $a_i/a_1$.

The junction fields are expressed by (3) through (6). Substituting (20), (21), (24), and (25) into them, and dividing by $a_1$, we obtain the following equations. In waveguide $a$

$$E_x = (1 + \rho)\sin(\pi y/w) + \sum_{i=2}^{M} \frac{a_i}{a_1}\sin(p\pi y/w) \tag{34}$$

$$H_y = (1 - \rho)y_{a1}\sin(\pi y/w) + \sum_{i=2}^{M} \frac{a_i}{a_1} y_{ai}\sin(p\pi y/w), \tag{35}$$

and in waveguide $b$ within $0 < y/w < 0.5(1 - t/w)$

$$E_x = \sum_{j=1}^{N} \frac{b_j}{a_1}\sin\left(\frac{2q\pi y/w}{1 - t/w}\right) \tag{36}$$

$$H_y = \sum_{j=1}^{N} \frac{b_j}{a_1} y_{bj}\sin\left(\frac{2q\pi y/w}{1 - t/w}\right). \tag{37}$$

When $0.5(1 + t/w) < y/w < 1$, substitute $(1 - y/w)$ for $y/w$ in (36) and (37). These fields are plotted (by computer) in Figs. 6 to 9 for half the guide width only, the fields being symmetrical about $y/w = 0.5$. Solid curves represent the field summation in guide $a$ immediately preceding the junction, and the broken curves represent the fields just inside guide $b$.

First of all, consider the electric fields. The quality of the match is seen to improve as more modes are used. Notice that the electric field in $b$ is zero at the vane. This is because each constituent mode of the Fourier series has zero electric field there. However, the summation of modes in guide $a$ does not vanish there, although it is attempting to do so. In particular, over the thick vane, $E_x$ in guide $a$ oscillates about zero. The greater the number of modes used, the greater the frequency of oscillation, and the smaller their amplitudes, converging to zero in the limit.

The aperture electric fields are roughly what one might have expected. The resulting pattern is a compromise between the incident $H_{01}$ mode and the requirement that the electric field should disappear at the vane; the maximum electric field does not occur at the center of the bifurcated region but slightly more to the center of the guide. As the wave proceeds down the guide, the higher-order modes attenuate very rapidly, and the pattern becomes substantially that of an undistorted half-sine wave in each region.

The magnetic field has to cope with a singularity at the edge of the vane. For this reason, $H_y$ does not attain as good a match as does $E_x$ for the same number of modes. Besides going to infinity as the corner is approached, an added difficulty is that $H_y$ in guide $b$ must vanish at the vane for the same reasons as $E_x$. This is attempted by rising to a high value near the vane, and then suddenly dropping sharply to zero.

In the limit, with increasingly large expansions, the oscillations disappear and $H_y$ increases almost linearly with $y/w$, except in the vicinity of the edge where it goes to infinity. Directly in front of the vane, a magnetic field exists supported by surface currents.

In the preceding study, the number of modes employed in guides $a$ and $b$ were equal, i.e., $M = N$. For several vane thicknesses ($t/w = 0$, 0.2, and 0.8), computations were made of input admittance $y'$ versus $N$ for a range of $M/N$ values. It was found that if $M/N$ was greater than unity, higher accuracy could be achieved. However, if $M/N$ was too large, instabilities occurred and wrong answers resulted. It is felt that there may be a way of choosing an optimum ratio for a given discontinuity, but the matter has not yet been investigated. In a general way, it seems that the greater the discontinuity, the larger the optimum $M/N$ ratio required.

### B. Finite-Length Bifurcation

Having considered the semi-infinite bifurcation, the finite bifurcation of length $l$ will now be studied. This is a symmetric problem, and so it will be treated as described in Section V.

The propagation constant of the $j$th mode in guide $b$ is given by

$$\gamma_j = \frac{\pi}{w}\sqrt{\left(\frac{2q}{1 - t/w}\right)^2 - \left(2\frac{w}{\lambda_0}\right)^2}. \tag{38}$$

The normalized input admittance of the $j$th mode, distance $l/2$ from an open circuit at the central plane, is

$$y'_{bj} = \tanh(\gamma_j l/2) \tag{39}$$

and with a short circuit at the central plane,

$$y'_{bj} = \coth(\gamma_j l/2). \tag{40}$$

$s_{jj}$ is then computed from (19). It could equally have been found by rewriting (18) to give

$$s_{jj} = \pm e^{-\gamma_j l}, \tag{41}$$

where the plus and minus signs correspond to symmetrical and antisymmetrical excitation, respectively.

Assuming an open circuit at the central plane, $\rho$ was computed from (12) and (13) (using the relevant values of $s_{jj}$), and from it the normalized input impedance $Z_{11} + Z_{12}$ was found. With a short circuit at the central plane, the input impedance $Z_{11} - Z_{12}$ was found. $Z_{12}$ was then easily calculated.

Table III presents the resulting equivalent $T$ network values for different normalized lengths $l/w$. For long vanes, $l/w \geq 10$, $Z_{11} - Z_{12}$ is the inverse of $y'$ computed for the semi-infinite case. As the length decreases, $Z_{11} - Z_{12}$ becomes smaller and $Z_{12}$ increases. At about $l/w = 0.1$, they are approximately equal. With further reduction in length, the bifurcation appears to be a zero-thickness inductive strip. Certain numerical difficulties arise when $l/w$ is made exactly equal to zero. This is heralded by increasing disagreement between the $Z_{12}$ values, computed for the $N = 25$ and $N = 50$ cases, as the length decreases. Finally, the results make no sense at all. Possibly, the simultaneous equations tend to become ill-conditioned in the limit. This point should be investigated more carefully.

TABLE I

SEMI-INFINITE BIFURCATIONS $w/\lambda_0 = 0.7$. NORMALIZED INPUT ADMITTANCE $y'$

| $N$ | $t/w = 0$ | $t/w = 0.2$ |
|---|---|---|
| 5 | $-j2.363$ | $-j7.213$ |
| 10 | $-j2.396$ | $-j7.335$ |
| 20 | $-j2.410$ | $-j7.378$ |
| 40 | $-j2.415$ | $-j7.394$ |

TABLE II

SEMI-INFINITE BIFURCATION $t/w = 0$, $w/\lambda_0 = 0.7$. FIRST FIVE FORWARD-SCATTERED MODE COEFFICIENTS $b_j/a_1$

| $j$ | $N = 5$ | $N = 10$ | $N = 20$ | $N = 40$ |
|---|---|---|---|---|
| 1 | 0.7956/67.06° | 0.7857/67.35° | 0.7824/67.46° | 0.7813/67.50° |
| 2 | −0.1802/67.06° | −0.1717/67.35° | −0.1693/67.46° | −0.1685/67.50° |
| 3 | 0.0975/67.06° | 0.0872/67.35° | 0.0847/67.46° | 0.0840/67.50° |
| 4 | −0.0715/67.06° | −0.0562/67.35° | −0.0535/67.46° | −0.0528/67.50° |
| 5 | 0.0789/67.06° | 0.0409/67.35° | 0.0379/67.46° | 0.0372/67.50° |

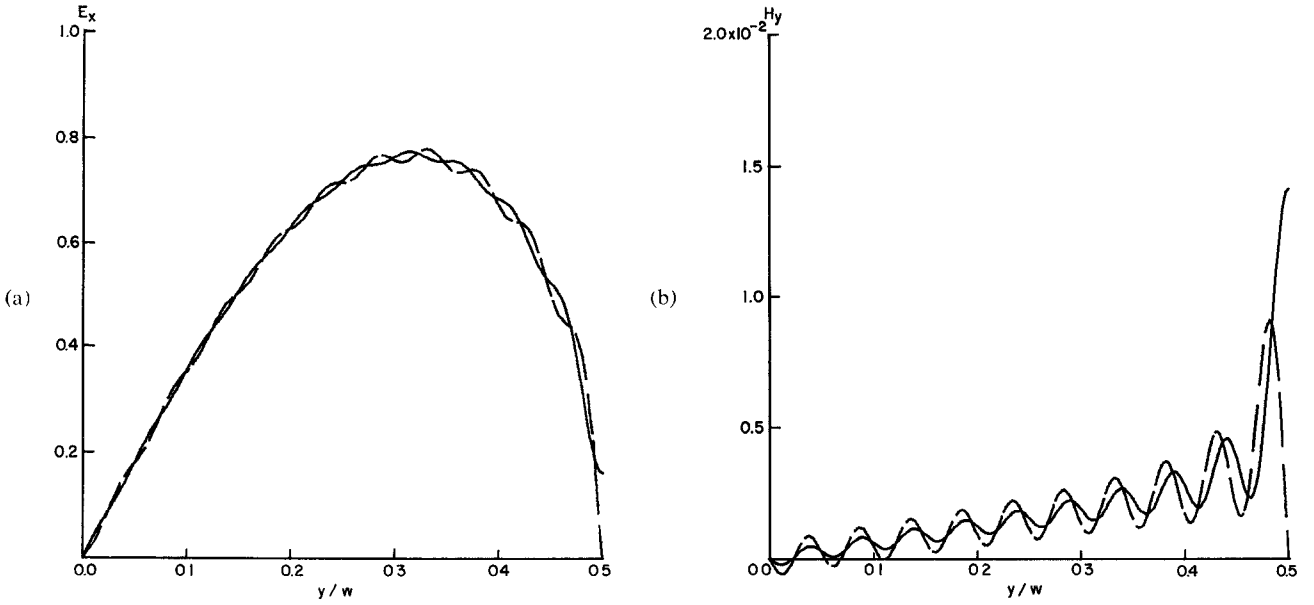


Fig. 6. $H$-plane bifurcation transverse fields: $t/w = 0$, $N = 20$. (a) Phase of $E_x = 67.46°$ (b) Phase of $H_y = -22.54°$.

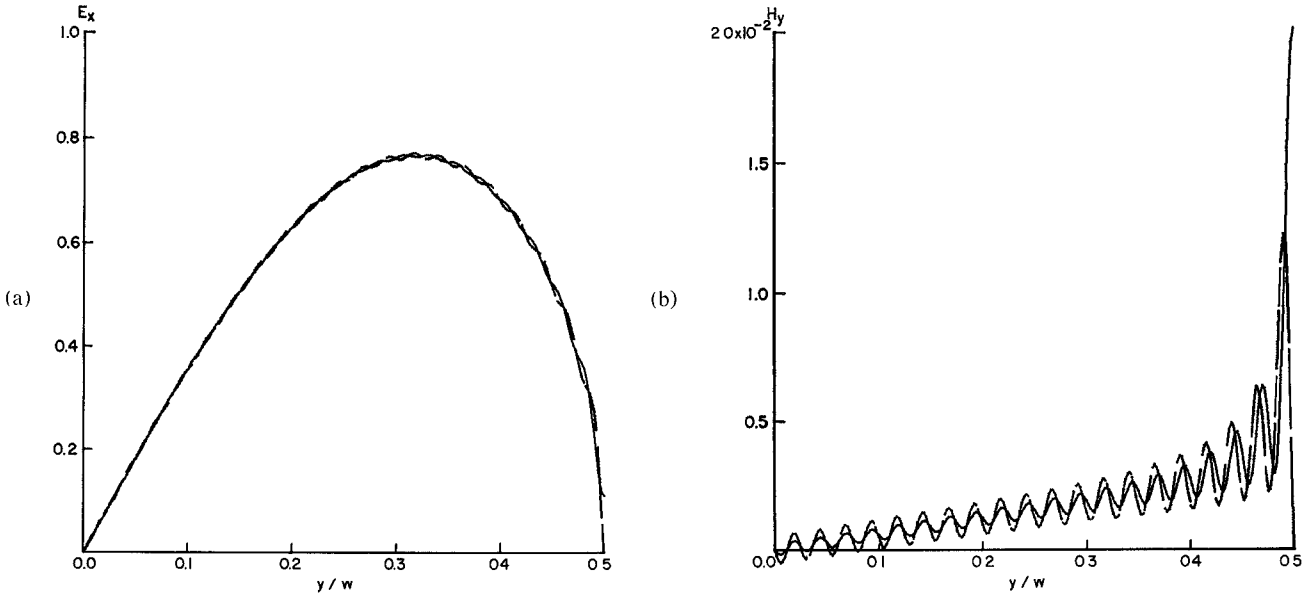


Fig. 7. $H$-plane bifurcation transverse fields: $t/w = 0$, $N = 40$. (a) Phase of $E_x = 67.50°$. (b) Phase of $H_y = -22.50°$.

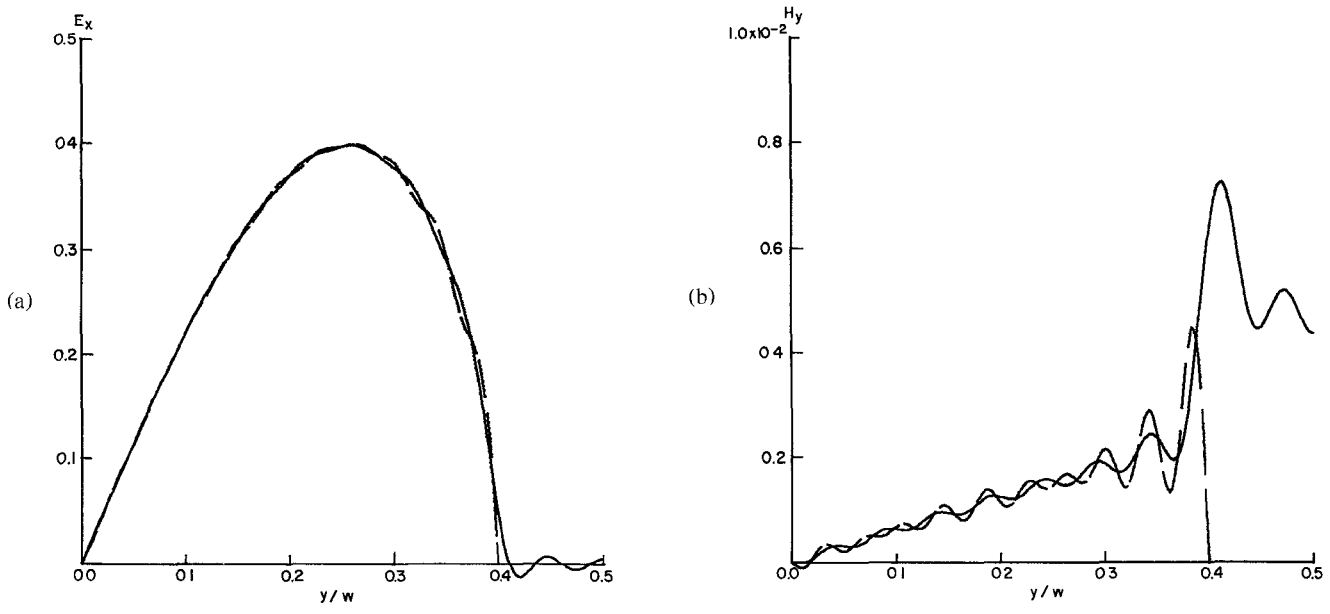


Fig. 8. $H$-plane bifurcation transverse fields: $t/w=0.2$, $N=20$. (a) Phase of $E_x=82.28°$. (b) Phase of $H_y=-7.72°$.

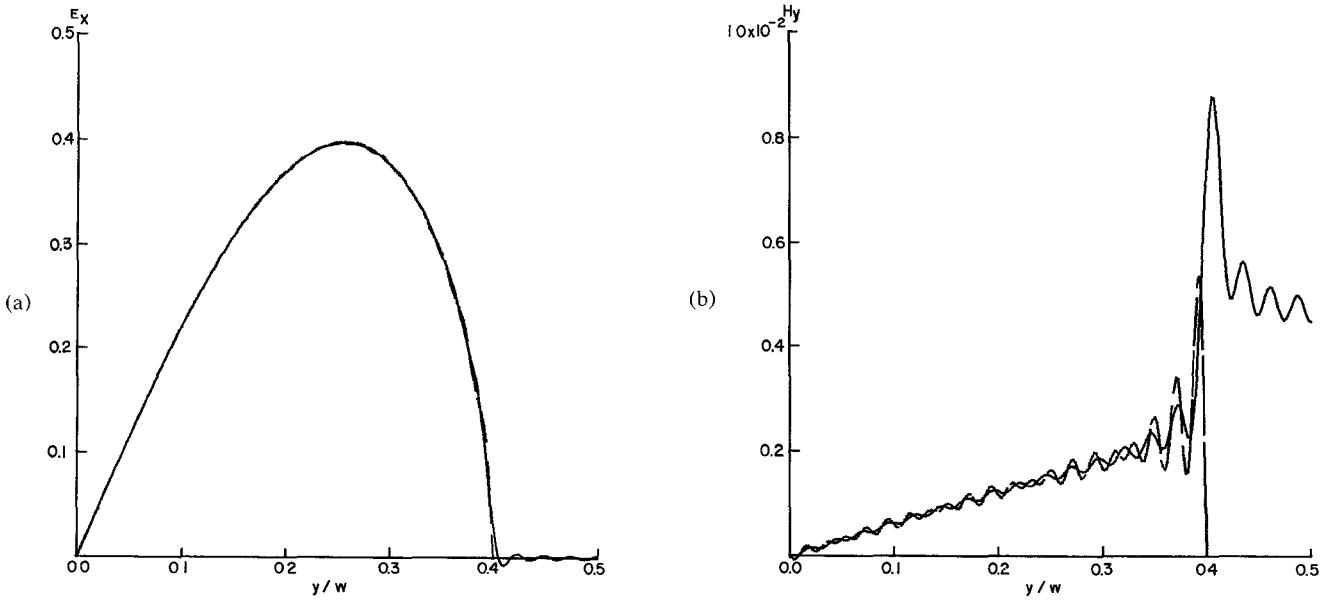


Fig. 9. $H$-plane bifurcation transverse fields: $t/w=0.2$, $N=40$. (a) Phase of $E_x=82.30$. (b) $H_y=-7.70°$.

TABLE III

FINITE-LENGTH BIFURCATION $t/w=0.2$, $w/\lambda_0=0.7$. SYMMETRICAL $T$ EQUIVALENT NETWORK PARAMETERS

| $l/w$ | $N=25$ | | $N=50$ | |
|---|---|---|---|---|
| | $Z_{12}$ | $Z_{11}-Z_{12}$ | $Z_{12}$ | $Z_{11}-Z_{12}$ |
| 10 | $j.0000$ | $j.1354$ | $j.0000$ | $j.1352$ |
| 1 | $j.0002$ | $j.1352$ | $j.0002$ | $j.1350$ |
| $10^{-1}$ | $j.0769$ | $j.0651$ | $j.0767$ | $j.0650$ |
| $10^{-2}$ | $j.1589$ | $j.0089$ | $j.1578$ | $j.0089$ |
| $10^{-3}$ | $j.1801$ | $j.0009$ | $j.1766$ | $j.0009$ |
| $10^{-4}$ | $j.1907$ | $j.0001$ | $j.1824$ | $j.0001$ |
| $10^{-5}$ | $j.1986$ | $j.0000$ | $j.1859$ | $j.0000$ |

## VII. Conclusions

A method was derived for solving a wide class of waveguide discontinuities by modal analysis. Thick and thin symmetrical $H$-plane bifurcations were studied. Input admittance and scattered modes were computed for a number of expansion sizes. Accuracy improved with the number of modes used.

Transverse electric-field patterns, plotted on both sides of the junction, indicated a good match for twenty and forty modes. Magnetic field matches less well due to the singularity at the vane. Even so, with forty modes the actual pattern may be easily discerned. Because permeable media do not exhibit singularities, it is believed that convergence will be much more rapid for discontinuities formed by them.

More information is required on the effects of different numbers of modes on alternate sides of a junction and on the solution's behavior as the axial length of a discontinuity vanishes.

## Acknowledgment

The author wishes to acknowledge the cooperation of the University of Manitoba Computer Centre. Particular appreciation is felt for the unstinting help of K. W. Schmidt who did the programming. Dr. J. W. Bandler contributed many helpful criticisms and ideas. Much of this work was developed while the author was with International Computers and Tabulators, Ltd., London. The cooperation of their Atlas programming group is gratefully acknowledged.

## References

[1] R. E. Collin, *Field Theory of Guided Waves*. New York: McGraw-Hill, 1960, pp. 409–452.
[2] L. Lewin, "On the resolution of a class of waveguide discontinuity problems by the use of singular integral equations," *IRE Trans. Microwave Theory and Techniques*, vol. MTT-9, pp. 321–332, July 1961.
[3] R. E. Collin [1], pp. 314–367.
[4] S. W. Drabowitch, "Multimode antennas," *Microwave J.*, vol. 9, pp. 41–51, January 1966.
[5] J. B. Davies and C. A. Muilwyk, "Numerical solution of uniform hollow waveguides and boundaries of arbitrary shape," *Proc. IEE* (London), vol. 113, pp. 277–284, February 1966.
[6] R. E. Collin [1], pp. 229–232.
[7] P. M. Morse and H. Feshbach, *Methods of Theoretical Physics*. New York: McGraw-Hill, 1953, pp. 928–929.
[8] C. E. Fröberg, *Introduction to Numerical Analysis*. Reading, Mass.: Addison-Wesley, 1965, pp. 172–201, 221–225.
[9] N. Marcuvitz, *Waveguide Handbook*. New York: McGraw-Hill, 1951, pp. 117–126.
[10] E. L. Ginzton, *Microwave Measurements*. New York: McGraw-Hill, 1957, pp. 317–329.
[11] C. E. Fröberg [8], pp. 74–75.
[12] N. Marcuvitz [9], pp. 172–174.

# A One-GHz Ferroelectric Limiter

JOHN B. HORTON, MEMBER, IEEE, AND MERLE R. DONALDSON, SENIOR MEMBER, IEEE

*Abstract*—**The design and analysis of a 1-GHz limiter which uses voltage variation of the dielectric constant of a ferroelectric material to achieve limiting is described. An RF electric field derived from the input power is used to change the relative dielectric constant $\varepsilon_r$ of the material; the resulting nonlinear change of capacitance of a small element of the material is used to change the condition of a tuned circuit. The tuned circuit terminates a quarter-wavelength stub which shunts the main transmission line, thereby providing a power-dependent mismatch at the junction of the two transmission lines. The degree of this mismatch is controlled by the condition of the tuned circuit and, therefore, the magnitude of the input power.**

**Theoretical analysis and experimental results for small signal and large signal operation are presented. Limiter analysis is based on the measured change of ferroelectric (nonlinear) capacitance as a function of dc electric field. The ferroelectric element is 0.011 by 0.013 by 0.020 (inches) machined from polycrystalline ($Pb_{0.315}$–$Sr_{0.685}$) $TiO_3$ material.**

Manuscript received November 9, 1966; revised May 10, 1967. The work reported here was performed at Sperry Microwave Electronics Co. (a Division of Sperry Rand Corp.), Clearwater, Fla., and was sponsored by the U. S. Army Electronics Command, Ft. Monmouth, N. J., under Contract DA36-039-AMC-03240(E).

J. B. Horton is with the Semiconductor Research and Development Laboratory, Texas Instruments Incorporated, Dallas, Tex. He was formerly with Sperry Microwave Electronics Company.

M. R. Donaldson is with the Electrical and Electronics Systems Department, University of South Florida, Tampa, Fla., and is a Consultant to Sperry Microwave Electronics Co.

FERROELECTRIC materials have inherent properties which cause the dielectric constant of the material to change as a function of ambient temperature and electric field. The change of dielectric constant with electric field is particularly interesting to circuit designers, since it represents a mechanism by which circuit response can be changed electrically. Applications to be considered at microwave frequencies are switches, harmonic generators, limiters, parametric amplifiers, phase shifters, etc. To date, a UHF limiter [1], an $X$-band harmonic generator [2], a UHF phase shifter [3], and an $L$-band switch [4], [5] have been reported, and parametric amplifiers have been investigated quite thoroughly [6]. The $L$-band passive limiter described here is a result of further effort to apply